Journal Pre-proof

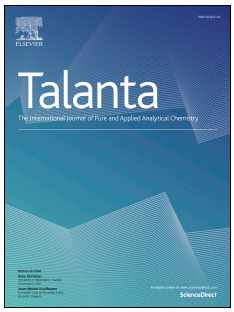

Genosensor made with a self-assembled monolayer matrix to detect *MGMT* gene methylation in head and neck cancer cell lines

Olivia Carr, Paulo A. Raymundo-Pereira, Flávio M. Shimizu, Bruna Pereira Sorroche, Matias Eliseo Melendez, Rafael de Oliveira Pedro, Paulo B. Miranda, André Lopes Carvalho, Rui M. Reis, Lídia M.R. B. Arantes, Osvaldo N. Oliveira, Jr.

PII: S0039-9140(19)31242-1

DOI: https://doi.org/10.1016/j.talanta.2019.120609

Reference: TAL 120609

To appear in: *Talanta*

Received Date: 5 November 2019

Revised Date: 28 November 2019

Accepted Date: 30 November 2019

Please cite this article as: O. Carr, P.A. Raymundo-Pereira, Flá.M. Shimizu, B.P. Sorroche, M.E. Melendez, R. de Oliveira Pedro, P.B. Miranda, André.Lopes. Carvalho, R.M. Reis, Lí.M.R.B. Arantes, O.N. Oliveira Jr., Genosensor made with a self-assembled monolayer matrix to detect *MGMT* gene methylation in head and neck cancer cell lines, *Talanta* (2020), doi: https://doi.org/10.1016/j.talanta.2019.120609.

Genosensor made with a self-assembled monolayer matrix to detect *MGMT* gene methylation in head and neck cancer cell lines

Olivia Carr[1], Paulo A. Raymundo-Pereira[1], Flávio M. Shimizu[1,a], Bruna Pereira Sorroche[2], Matias Eliseo Melendez[2], Rafael de Oliveira Pedro[1], Paulo B. Miranda[1], André Lopes Carvalho[2], Rui M. Reis[2,3,4], Lídia M. R. B. Arantes[2], Osvaldo N. Oliveira Jr[1*]

[1] São Carlos Institute of Physics, University of São Paulo, 13566-590 São Carlos, Brazil

[2] Molecular Oncology Research Center, Barretos Cancer Hospital, 14784-400 Barretos, Brazil

[3]Life and Health Sciences Research Institute (ICVS), School of Medicine, University of Minho, Braga, Portugal;

[4]ICVS/3B's - PT Government Associate Laboratory, Braga/Guimarães, Portugal.

[a]Present address: Brazilian Nanotechnology National Laboratory (LNNano), Brazilian Center for Research in Energy and Materials (CNPEM), 13083-970, Campinas, SP, Brazil.

*Corresponding author:

São Carlos Institute of Physics and São Carlos Institute of Chemistry, University of São Paulo (USP), CP 369, CEP 13560–970, São Carlos, São Paulo, Brazil

E-mail address: chu@ifsc.usp.br (Osvaldo N. Oliveira Jr.)

Tel.: +55 16 33518098; fax: +55 16 33518350.

Graphical abstract

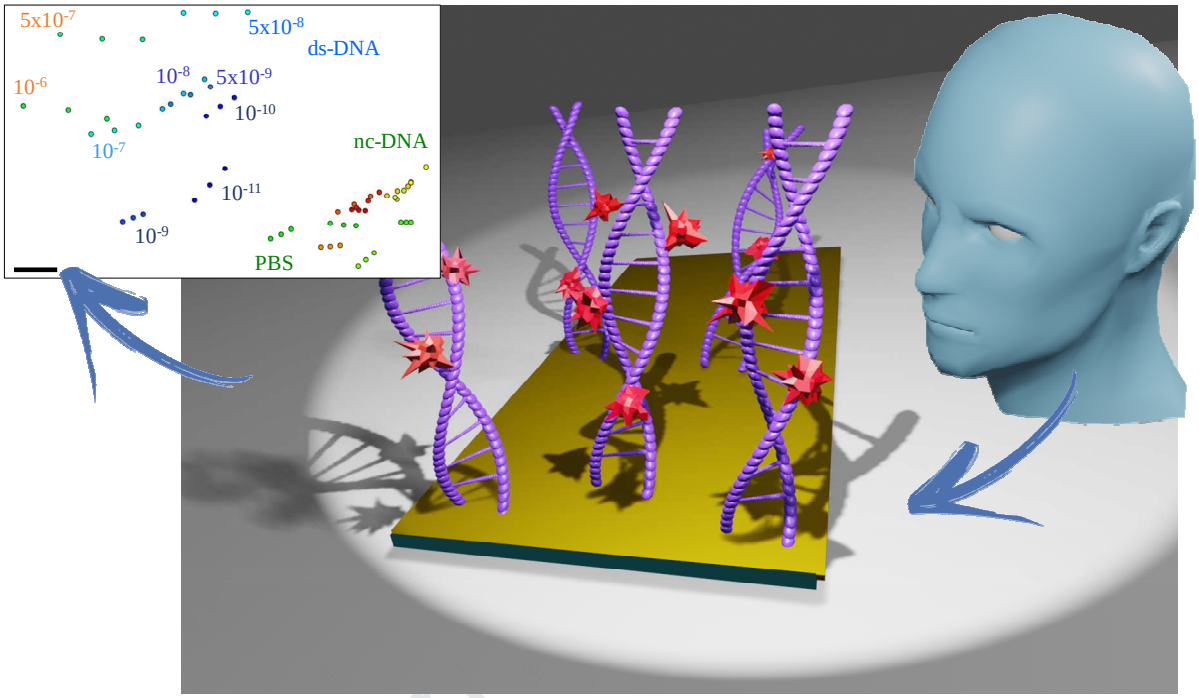

Genosensor made with a self-assembled monolayer matrix to detect *MGMT* gene methylation in head and neck cancer cell lines

Olivia Carr[1], Paulo A. Raymundo-Pereira[1], Flávio M. Shimizu[1,a], Bruna Pereira Sorroche[2], Matias Eliseo Melendez[2], Rafael de Oliveira Pedro[1], Paulo B. Miranda[1], André Lopes Carvalho[2], Rui M. Reis[2,3,4], Lídia M. R. B. Arantes[2], Osvaldo N. Oliveira Jr[1*]

[1] São Carlos Institute of Physics, University of São Paulo, 13566-590 São Carlos, Brazil

[2] Molecular Oncology Research Center, Barretos Cancer Hospital, 14784-400 Barretos, Brazil

[3]Life and Health Sciences Research Institute (ICVS), School of Medicine, University of Minho, Braga, Portugal;

[4]ICVS/3B's - PT Government Associate Laboratory, Braga/Guimarães, Portugal.

[a]Present address: Brazilian Nanotechnology National Laboratory (LNNano), Brazilian Center for Research in Energy and Materials (CNPEM), 13083-970, Campinas, SP, Brazil.

*Corresponding author:

São Carlos Institute of Physics and São Carlos Institute of Chemistry, University of São Paulo (USP), CP 369, CEP 13560–970, São Carlos, São Paulo, Brazil

E-mail address: chu@ifsc.usp.br (Osvaldo N. Oliveira Jr.)

Tel.: +55 16 33518098; fax: +55 16 33518350.

ABSTRACT

DNA methylation is involved in the oncogenesis of head and neck squamous cell carcinoma and could be used for early detection of cancer to increase the chances of cure, but unfortunately diagnosis is usually made at late stages of the disease. In this work we developed genosensors to detect DNA methylation of the *MGMT* gene in head and neck cancer cell lines. The probe for *MGMT* promoter methylation was immobilized on gold electrodes modified with 11-mercaptoundecanoic acid (11-MUA) self-assembled monolayers (SAM). Detection was performed with electrochemical impedance spectroscopy, with clear distinction between methylated from non-methylated DNA from head and neck cell lines. The genosensor is sensitive with a low detection limit of 0.24×10^{-12} mol L^{-1}. In addition, the cell lines FaDu, HN13, JHU28 and SCC25, which are non-methylated for the *MGMT* gene, could be distinguished from the HN13 cell line which has a high degree of *MGMT* methylation (97%), thus confirming the selectivity. Samples with different percentages of *MGMT* DNA methylation could be separated in multidimensional projections using the visualization technique interactive document mapping (IDMAP). The genosensor matrix and the immobilization procedures are generic, and can be extended to other DNA methylation biomarkers.

Keywords: DNA methylation, Head and neck cancer, Genosensor, Impedance spectroscopy, *MGMT* gene, Biosensor.

1. Introduction

Head and neck cancers represent the eighth most prevalent worldwide, with 830,000 new cases and 430,000 deaths per year [1]. It is thus essential to develop methodologies for detecting the disease at an early stage to reduce mortality through proper therapeutic management. Early cancer detection can in principle be made with immunoassays [2–5] employing antigen-antibody reactions, but their applicability requires prior existence of the disease for the proper biomarkers be expressed. Methods based on gene monitoring, on the other hand, can provide detection at even earlier stages. These methods exploit the fact that cancer arises from genetic and epigenetic alterations, such as DNA methylation (addition of methyl groups – CH_3) [6]. The increase in methylation at the promoter region of a tumor suppressor gene usually leads to gene inactivation, responsible for repairing DNA damage, detoxification, cell cycle regulation and apoptosis [7,8]. Approximately 5% of the promoter region of genes are hypermethylated in solid tumors [9]. The process of carcinogenesis in head and neck tumors, whether by the mutagenic action of tobacco and alcohol or mediated by human papilloma virus (HPV) infection, consists of multiple steps, in which genetic and epigenetic changes accumulate [10]. Epigenetic changes are inherited during cell division and lead to modifications in the phenotype, without changes in the DNA sequence [11].

Methylation of gene promoters is a potential molecular marker for several tumors [6], being an early event of carcinogenesis in head and neck tumors that can be detected in precursor lesions. Disease severity and metastasis are correlated with hypermethylation of gene promoters, with a high frequency in the promoter region of the $P16^{INK4A}$ gene in primary head and neck squamous cell carcinomas (HNSCC) [12]. There is also correlation between the hypermethylation profile of *CCNA1* (cyclin A1), *DAPK* (death-associated protein kinase), *DCC*

(deleted in colorectal cancer), *MGMT* (o^6-methylguanine DNA methyltransferase) and *TIMP3* (metalloproteinase inhibitor 3) genes with histological characteristics of oral carcinomas, with loss of *DAPK* expression associated with hypermethylation [13]. An evaluation in the promoter region of nine genes in oral cavity cancer showed a strong link between clinicopathological aspects and the methylation of at least six of these genes [13]. Conventional methods to gene monitoring, including quantitative methylation-specific polymerase chain reaction (PCR) analyses (Q-MSP), are expensive and time consuming. As an alternative, electrochemical devices have been applied as genosensors for this analytical task [14]. They are attractive due to the ease with which sensitive, selective genosensors can be obtained which are amenable to miniaturization and operation with small volumes [15–17].

In this paper, we present a genosensor containing a *MGMT* promoter methylation probe sequence [8], capable of detecting DNA methylation in this gene through electrochemical impedance spectroscopy (EIS). Gold electrodes modified with self-assembled monolayers (SAM) of mercaptoacetic acid (MAA) and 11-mercaptoundecanoic acid (MUA) were employed as platforms to immobilize the DNA methylation probe. Polarization-modulated infrared reflection-absorption spectroscopy (PM-IRRAS), contact angle and electrochemical impedance spectroscopy (EIS) were used to characterize the genosensor architecture and determine molecular-level interactions in detecting DNA methylation with a complementary sequence to the probe. High sensitivity was obtained, which also allowed to distinguish cell samples with distinct percentages of DNA methylation.

2. Experimental section

The gold (Au) electrodes were produced at the Brazilian National Nanotechnology

Laboratory (LNNano/CNPEM). First, microscope glass slides were washed with neutral detergent to remove impurities and rinsed in ultrapure water, ethanol and dried under N_2 gas flow. The slides were coated with 20 nm of chromium, as adhesive layer, and then 150 nm Au-layer by sputtering (Balzers BA510). Before use in analytical tasks, Au electrodes were chemically cleaned in Piranha solution (H_2SO_4 and H_2O_2 at 1:1 (v/v)) for 30 min and electrochemically cleaned in 0.1 M H_2SO_4 solution by cyclic voltammetry in a potential range from 0 to 0.9 V at scan rate of 1 V/s for 60 cycles. Ultrapure water (resistivity >18.2 MΩ cm) was collected from a Millipore Direct-Q5 system (Billerica, USA).

The electrodes shown in Fig. 1 have dimensions of 2.5 x 0.7 cm, with active area of 0.9 cm^2, delimited by a double-sided tape. The genosensors consisted of Au electrodes coated with a self-assembled monolayer (SAM) [18] of either mercaptoacetic acid (MAA) (50×10^{-3} mol L^{-1}) or 11-mercaptoundecanoic acid (11-MUA) (50×10^{-3} mol L^{-1}). Distinct immersion times were used to adsorb MAA or MUA, and optimized genosensors were obtained with 24 h 11-MUA in ethanol at room temperature (ultrapure water was also used). The activation of COOH thiol sites was performed with a solution of 400×10^{-3} mol L^{-1} of 1-ethyl-3-[3-dimethylaminopropyl] carbodiimide hydrochloride (EDC) and 100×10^{-3} mol L^{-1} of N-hydroxysuccinimide (NHS) for 30 min at room temperature in water to enable DNA probe immobilization. These electrodes were immersed for 24 h at room temperature in a 1×10^{-3} mol L^{-1} PBS/$MgCl_2$ solution (1.0×10^{-6} mol L^{-1}) containing the NH_2-ssDNA probe. The final step in the genosensor preparation involved immersion in 1.0×10^{-3} mol L^{-1} ethanolamine solution (Sigma-Aldrich) as a blocker of active sites to avoid non-specific adsorption. 11-MUA, MAA, EDC, NHS and ethanolamine were acquired from Sigma-Aldrich. Fig. 1 depicts schematically the film architecture and the detection step of the genosensor.

Fig. 1

The methylated DNA sequences to be detected were prepared in phosphate buffered saline (PBS) solution consisting of 137×10^{-3} mol L^{-1} NaCl, 10×10^{-3} mol L^{-1} $Na_2.HPO_4$, 1.7×10^{-3} mol L^{-1} $KH_2.PO_4$, 2.7×10^{-3} mol L^{-1} KCl (pH 7.4) with addition of 1.0×10^{-3} mol L^{-1} $MgCl_2$. These reagents were purchased from Synth (Brazil). The *MGMT* methylated DNA sequences used as probe and target were synthesized by Sigma-Aldrich, as indicated in Table 1:

Table 1. Probe, complementary sequence, sequence with one base exchange, and non-complementary DNA sequence.

	Bases	Sequence
DNA methylation probe (NH_2-ssDNA)	24	5' - NH_2-$(CH_2)_6$ – TTT CGC AAA CGA TAC GCA CCG CGA – 3'
Complementary sequence (ds-DNA)	21	5' – TCG CGG TGC GTA TCG TTT GCG – 3'
Complementary sequence with 1 base exchanged (1b-DNA)	21	5' – TCG CGG TGC G**G**A TCG TTT GCG – 3'
Non-complementary sequence (nc-DNA)	21	5' – CGA GAA CTT ACG GTC CCC TTA – 3'

Detection experiments were performed with complementary and non-complementary sequences in a concentration range between 1.0×10^{-12} and 1.0×10^{-6} mol L^{-1} diluted in PBS/$MgCl_2$ solutions. The optimized hybridization process was performed at 86 °C for 1 h, followed by being placed on ice for 5 min. The choice of this temperature was made taking the melting temperature (Tm) as reference and adding 10 °C. The Tm value is important for several techniques in molecular biology, being defined as the temperature in which 50% of the oligonucleotides are duplexed with their complementary sequence while the remaining 50% are free in solution. In the electrochemical characterization, 5.0×10^{-3} mol L^{-1} of potassium-ferrocyanide and -ferricyanide ($K_3[Fe(CN)_6]/K_4[Fe(CN)_6]$) (Sigma-Aldrich) dissolved in 1.0×10^{-3} mol L^{-1} PBS/$MgCl_2$ solution were used. Measurements were also performed for the head

and neck cancer cell lines with distinct degrees of methylation, *viz*. HN13 (97% methylation), JHU28 (93%), Fadu (3%), and SCC25 (2%). DNAs from head and neck cell lines were modified with sodium bisulphite and stored at –80 °C. The sodium bisulphite conversion was carried out using EpiTect Bisulphite Kit (*Qiagen*, Valencia, CA), according to the manufacturer's recommendation. When the complementary DNA was incubated with sodium bisulphite, the unmethylated cytosine residues were converted into uracil and later in thymine, leaving methylated cytosines unchanged. Hence, different DNA sequences were obtained for methylated and non-methylated DNA. Prior to the detection measurements, the DNAs were thermally treated at 95 °C for 5 min to open the double strands, followed by being placed on ice for 1 min.

The electrochemical measurements were performed in a potentiostat/galvanostat Autolab PGSTAT 204 equipped with FRA module controlled by Nova 2.0 software (Metrohm) using a conventional three-electrode system: gold, Ag/AgCl, and platinum plate (1.0 cm^2) as working, reference and auxiliary electrodes, respectively. Electrochemical impedance spectroscopy was applied in the frequency range between 100 kHz and 0.1 Hz under an a.c. voltage amplitude of 10 mV. The whole impedance spectra were processed with the multidimensional projection technique named Interactive Document Mapping (IDMAP) [19], implemented in the PEx-Sensors software [20]. In this technique, each spectrum is represented as a point in the 2D projected plot.

Sum-Frequency Generation Vibrational Spectroscopy (SFG) is a surface-specific optical technique. It gives information about composition and orientation of interfacial molecules. More details on this technique can be found elsewhere [20-22]. The organization of the matrix of the genosensor was probed by measuring the sum-frequency generation (SFG) spectra in a commercial SFG setup (EKSPLA, Lithuania) described in [23]. The beams of two pulsed lasers

were made to overlap spatially and temporally on the sample surface. The 532 nm laser (VIS) had ~60 μJ per pulse while the tunable infrared (IR) within the range from 1200 to 1600 cm^{-1} had ~50-120 μJ per pulse. They were generated with a pulse duration of ~30 ps and at a repetition rate of 20 Hz and focused on the sample surface with angles of incidence of 55º (IR, spot size ~0.7 mm) and 60º (VIS, spot size ~1.5 mm). Due to the gold surface selection rules, only polarization combinations containing the polarized p-polarized IR beam generate SFG signal with appreciable intensity. The SFG spectra were taken with PPP polarization (p-polarized SFG, p-polarized VIS and p-polarized IR) from 1200 to 1600 cm^{-1}. Each point in the spectrum represents the average of 100 pulses with an increment of 3 cm^{-1}. The data were modeled using resonances with Lorentzian line profiles [21]. The film characterization and detection were also investigated using polarization-modulated infrared reflection absorption spectroscopy (PM-IRRAS) with a model KSV PMI 550 apparatus (KSV, Helsinki, Finland), with a spectral resolution of 8 cm^{-1} and an incidence angle of 80°.

3. Results and discussion

Hybridization of complementary sequences in a genosensor may be highly dependent on the organization of immobilized DNA probes [24], and therefore a suitable matrix for depositing the active layer containing DNA probes is required. Here SAMs made with two mercapto acids prepared either in aqueous or ethanol solutions were evaluated. The MAA-based genosensor failed to detect the complementary sequences of NH_2-ssDNA probe, and this failure was attributed to the lack of organization of the matrix. This was inferred from subsidiary experiments with SFG spectroscopy, whose results are shown in Fig. S1 in the Supporting Information, where one notes that an organized MAA SAM was only obtained if the adsorption

time was 30 days or more. In contrast, MUA SAMs are well organized even when prepared within 24 h [25], then serving to fabricate successful genosensors. The negative peak at 1255 cm^{-1} in the SFG spectra of Fig. S1 d and e is attributed to C-OH stretching of the carboxylic acid group of MAA [26]. It interferes destructively with the non-resonant gold background, indicating a net (upward) orientation of –COOH of MAA molecules. It is worth mentioning that the absence of a signal in the SFG spectra for shorter adsorption times does not imply absence of molecules on the gold surface, but a lack of net orientation. MAA molecules probably adsorb to the surface of gold quickly, but they need a long time to reach sufficient organization to be observable in the SFG spectra. These results suggest that MAA SAM will have an appreciable degree of organization only after 30 days of adsorption.

The optimized genosensor with the NH_2-ssDNA probe immobilized on a MUA SAM was used to detect distinct concentrations of the complementary DNA (ds-DNA) and non-complementary DNA (nc-DNA). Fig. 2a shows the electrochemical impedance spectra with the impedance increasing with the concentration of the complementary sequence mainly at low frequencies (between 0.1 to 100 Hz), which is the region governed by changes in the electrical double layer. This was expected because the hybridization between the complementary sequence and the probe occurs on the genosensor surface. The results for the non-complementary sequences in Fig. 2b indicate small changes with concentration, probably due to non-specific interactions. Similar dependences on the concentration for the complementary and non-complementary sequences are noted in the Nyquist plots in Fig. S2 in the Supporting Information.

Fig. 2

The concentration dependence of the impedance spectra can be better visualized by plotting the change in impedance – in comparison with the value for the reference ethanolamine (Z_0) coating – at a fixed frequency. The changes in impedance ($Z-Z_0$) of complementary (ssDNA-red dots) and non-complementary (nc-DNA-black dots) sequences at 1 Hz are shown in Fig. 3. The analytical curve is linear with the logarithm of ssDNA concentration, while negligible changes were observed for nc-DNA. For NH_2-ssDNA, the linear concentration range between 1.0×10^{-11} and 5.0×10^{-8} mol L^{-1}, and between 1.0×10^{-8} and 1.0×10^{-6} mol L^{-1} can be fitted with the regression equation $(Z-Z_0) = 199{,}150.21 + 15{,}772.64 \log C$ and $(Z-Z_0) = 517{,}319.07 + 54{,}125.61 \log C$, where C is ssDNA concentration, respectively. The detection limits are 0.24×10^{-12} and 277×10^{-12} mol L^{-1} for the two linear ranges, estimated using $\mathrm{LOD} = 3SD/\theta$, with θ being the slope and SD the standard deviation of the linear regression [27]. The increase in impedance for ds-DNA is explained by hybridization with the probe (NH_2-ssDNA), which forms a double helix structure via binding on the electronegative phosphate groups on the surface exposed. This makes it difficult for the $[Fe(CN)_6]^{-3/-4}$ species to reach the electrode due to electrostatic repulsion, thus increasing the impedance values.

Fig. 3

Table 2 compares the figures of merit of the genosensor reported here with those from the few sensing platforms in the literature for detection of gene-specific methylation. Only the biosensor by Cai and co-workers [28] had a smaller LOD than the genosensor presented in this paper. However, biosensing in ref. [28] involved the use of gold nanoparticles and antibodies requiring long times of preparation. This is in contrast to the protocol described here, which is simple and some sophistication only exists in the analysis method. Furthermore, we shall show that the sensitivity is adequate to detect the target gene-specific methylation in cell samples.

Table 2: Electrochemical biosensing strategies for determination of DNA methylation.

Electrode	Fundamentals	Target	Technique	Range	LOD	Sample	Ref
Screen Printed Carbon SPCE)	Sandwich structure based on PNA probe and anti-5-mC antibody AuNPs and LPA for double signal amplification	Tumor-specific mutations and 5-mC methylation of PIK3CA gene	Square Wave Voltammetry	50 –10000 × 10^{-15}	10 × 10^{-15} mol L^{-1}	Spiked human plasma samples	[28]
Screen Printed Carbon (SPCE)	Immunopurification (anti-5-mC-MBs) Immunodetection(b DNA-Cp-MBs)	5-mC/global (anti-5-mC) and gene-specific (b-DNA-Cp-MBs, MGMT	Amperometry	Gene-specific: 5-mC: 4.0−250 × 10^{-12} (MGMT)	Gene-specific: 5-mC: 1.2 × 10^{-12} mol L^{-1} (MGMT)	gDNA extracted from cell lines paraffin-embedded tissues from CRCP and direct determination 1/5 diluted serum from breast and lung cancer patients	[29]
Glassy Carbon (GCE)	Choline ($HOCH_2CH_2N^+(CH_3)_3Cl$;Ch) monolayer supported gold nanoparticles film modified glassy carbon electrode (GCE) was designed as the electrode	p53 gene	Electrochemical Impedance Spectroscopy	50 × 10^{-12} – 96 × 10^{-9}	18 × 10^{-12} mol L^{-1}	p53 gene obtained from tumor cells	[30]

	interface for the immobilization of the PNA probe						
Gold (AuE)	Bisulfite + self-assembled tetrahedral DNA probes to capture amplicons generated by aMSP	5-mC/p16INK4a	Amperometry	$3 – 150 \times 10^{-12}$ g	One methylated DNA molecule in the presence of a 1000-fold excess of unmethylated alleles	cDNA extracted from plasma samples of lung cancer patients	[31]
Gold (AuE)	Self assembled MUA + amine DNA probe	5-mC/MGMT	Electrochemical Impedance Spectroscopy	$1.0 \times 10^{-11} – 1.0 \times 10^{-6}$ mol L^{-1}	0.24×10^{-12} mol L^{-1}	DNA extracted from cell lines from head and neck cancer	This work

The selectivity tests for the genosensor were performed for different DNA sequences, i.e. complementary sequence (ds-DNA), 1 base exchange (1b-DNA) and the non-complementary sequence (nc-DNA). The impedance spectra with 1 μM concentration of each sequence were analyzed by comparing the signal difference of the control sequences and the signal from the last sensor preparation step (NH_2-ssDNA/ethanolamine) ($Z-Z_0$). Fig. 4 shows the change in impedance ($Z-Z_0$) at 1 Hz. The complementary sequence (ds-DNA) generated a higher signal than the other sequences, consistent with hybridization of the two strands. The 1b-DNA sequence differs from the ds-DNA sequence by a guanine in the middle. Since this base is not complementary to the NH_2-ssDNA probe, hybridization is partial and the signal is smaller than for ds-DNA. As expected, the smallest variation was observed for nc-DNA.

Fig. 4

To validate the genosensor performance, we carried out methylation analysis using the pyrosequencing method (unpublished data; supplementary Fig. S3 and supplementary Table S1) in head and neck cell lines DNA, which presented different methylation patterns in the promoter region of *MGMT* gene: HN13 (97% methylation), JHU28 (93%), FaDu (3%), SCC25 (2%). They were provided by the Molecular Oncology Research Center in Barretos Cancer Hospital with different percentages of DNA methylation at a concentration of 0.2 ng/μL. Fig. 5 shows the impedance spectra of the hybridized methylated DNAs on the probe. The impedance increased with the percentage of methylation since with a higher amount of methylated cytosine the sequence approaches the complementary sequence (ds-DNA). This is because the methylated DNAs sequences undergo a treatment with sodium bisulphite that converts the unmethylated

cytosines into uracil and later into thymine, keeping methylated cytosine unchanged. Fig. 5b shows the difference in impedance for the methylated DNAs and the genosensor reference (i.e. the probe NH_2-ssDNA/ethanolamine) (Z-Z_0) at 1 Hz. The sample with the highest percentage of *MGMT* DNA methylation (HN13) is hybridized as it is the complementary sequence. The sample with the lowest percentage of methylation (SCC25) displayed the smallest change, as expected since it is the non-complementary sequence to the probe; hybridization does not occur in this case. A similar distinction of the cell lines could be observed in the Nyquist plots in Fig. S4 in the Supporting Information.

Fig. 5

In order to illustrate the ability of the genosensor in distinguishing the different types of samples, the IDMAP technique was used to plot the data from Fig. 2 and 5a. The resulting maps in Fig. 6 correspond to data for complementary and non-complementary DNA sequences (a) and head and neck cancer cell line DNA samples (b). The data points for nc-DNA samples are close to those of PBS, and the higher concentrations of ds-DNA are located further away. Also significant is that the distinct concentrations of ds-DNA can – for the most part - be distinguished from each other. In addition, the samples from the different cell lines are mapped on different places, with those with similar degrees of methylation being closer.

Fig. 6

We confirmed that the specific sensing of DNA complementary sequences is due to hybridization by measuring the PM-IRRAS spectra of the genosensor before and after the

sensing experiments. Fig. S5 in the Supporting Information shows the spectra in the 1600 to 1800 cm^{-1} region for the genosensor (i.e. NH_2-ssDNA), after the measurement with the complementary sequence (ds-DNA), and with the non-complementary sequence (nc-DNA). The three spectra exhibited the same 4 bands at 1622, 1646, 1694 and 1745 cm^{-1}. The 1622 cm^{-1} band is attributed to guanine NH_2 bending, the 1646 cm^{-1} band is assigned to cytosine ring deformation (C=N stretching), and the 1694 and 1745 cm^{-1} bands are assigned to stretching of thymine carbonyl [32]. One way to differentiate these spectra is to calculate the band area, for which the bands were deconvoluted with Gaussian functions. The bandwidth, area and position of the deconvoluted bands are shown in Table S2. The area of the 4 bands for the complementary sequence (ds-DNA) is smaller than that for the probe and non-complementary sequence due to formation of base pairs (A-T, C-G) with hydrogen bonds. The adenine NH_2 flexion movement becomes more restricted in the base pair and therefore the energy of NH_2 movement increases. The wavenumber of the thymine carbonyl stretching with hydrogen bonding at the base pair A-T decreased after base pair formation owing to the decrease in the C-O strength with the hydrogen bond. The areas under the spectra for the probe and non-complementary sequence are close, which means that hybridization with the non-complementary sequence has not occurred.

4. Conclusions

The organization of the matrix on which an active layer of DNA probes was adsorbed has been proven crucial for the successful detection of DNA methylation of *MGMT* gene in head and neck cancer cell lines. This was verified by comparing electrochemical impedance sensing data from genosensors made with two types of SAMs prepared in water and ethanol. Successful detection was only observed when the SAMs could be well ordered, according to SFG data. This

sensing platform allowed us to develop a genosensor able to identify, distinguish and measure the presence of an MGMT gene methylation using simple hybridization reactions under optimized conditions. The genosensor exhibited high sensitivity with a limit of detection of 0.24 × 10^{-12} mol L^{-1} within a wide concentration range from 1.0 × 10^{-11} to 1.0 × 10^{-6} mol L^{-1}. The selectivity of the genosensor was demonstrated by noting that the 1 base-exchange sequence (1b-DNA) displayed a smaller signal than the complementary sequence, while being larger than for the non-complementary sequence. Using the projection technique IDMAP, we could distinguish the impedance data from non-complementary and complementary DNA sequences, in addition to HNSCC cell lines with different percentages of *MGMT* DNA methylation. This approach can be used for future evaluation of *MGMT* methylation status in glioblastomas, where it constitutes an important biomarker of temozolomide response [28, 29]. The matrix and procedures employed in developing the genosensors reported here are generic, and may be replicated for other sequences in order to evaluate changes in DNA sequences at a low cost.

Acknowledgements

This work was supported by CNPq, INEO and FAPESP (2013/14262-7 and 2016/01919-6). The authors are grateful to Angelo Luiz Gobbi and Maria Helena de Oliveira Piazzetta (LMF/LNNano/CNPEM) for the gold electrodes.

References

[1] F. Bray, J. Ferlay, I. Soerjomataram, R.L. Siegel, L.A. Torre, A. Jemal, Global cancer statistics 2018: GLOBOCAN estimates of incidence and mortality worldwide for 36 cancers in 185 countries, CA. Cancer J. Clin. 68 (2018) 394-424.

[2] A.C. Soares, J.C. Soares, F.M. Shimizu, V. da C. Rodrigues, I.T. Awan, M.E. Melendez, M.H.O. Piazzetta, A.L. Gobbi, R.M. Reis, J.H.T.G. Fregnani, A.L. Carvalho, O.N. Oliveira, A simple architecture with self-assembled monolayers to build immunosensors for detecting the pancreatic cancer biomarker CA19-9, The Analyst 143 (2018) 3302–3308.

[3] J.C. Soares, A.C. Soares, P.A.R. Pereira, V. da C. Rodrigues, F.M. Shimizu, M.E. Melendez, C. Scapulatempo Neto, A.L. Carvalho, F.L. Leite, S.A.S. Machado, O.N. Oliveira, Adsorption according to the Langmuir–Freundlich model is the detection mechanism of the antigen p53 for early diagnosis of cancer, Phys. Chem. Chem. Phys. 18 (2016) 8412–8418.

[4] D.E. Camilo, C.M. Miyazaki, F.M. Shimizu, M. Ferreira, Improving direct immunoassay response by layer-by-layer films of gold nanoparticles – Antibody conjugate towards label-free detection, Mater. Sci. Eng. C. 102 (2019) 315-323.

[5] C.A. Proença, T.A. Baldo, T.A. Freitas, E.M. Materón, A. Wong, A.A. Durán, M.E. Melendez, G. Zambrano, R.C. Faria, Novel enzyme-free immunomagnetic microfluidic device based on Co0.25Zn0.75Fe2O4 for cancer biomarker detection, Anal. Chim. Acta. 1071 (2019) 59–69.

[6] H. Fayazfar, A. Afshar, M. Dolati, A. Dolati, DNA impedance biosensor for detection of cancer, TP53 gene mutation, based on gold nanoparticles/aligned carbon nanotubes modified electrode., Anal. Chim. Acta. 836 (2014) 34–44.

[7] L.M.R.B. Arantes, A.C. de Carvalho, M.E. Melendez, A.L. Carvalho, E.M. Goloni-Bertollo, Methylation as a biomarker for head and neck cancer., Oral Oncol. 50 (2014) 587–92.

[8] L.M.R.B. Arantes, A.C. De Carvalho, M.E. Melendez, C.C. Centrone, J.F. Góis-Filho, T.N. Toporcov, D.N. Caly, E.H. Tajara, E.M. Goloni-Bertollo, A.L. Carvalho, Validation of methylation markers for diagnosis of oral cavity cancer, Eur. J. Cancer. 51 (2015) 632–641.

[9] A. Zhu, D. Lee, H. Shim, Metabolic positron emission tomography imaging in cancer detection and therapy response, Semin. Oncol. 38 (2011) 55–69.

[10] K. Strati, P.F. Lambert, Human papillomavirus association with head and neck cancers: Understanding virus biology and using it in the development of cancer diagnostics, Expert Opin. Med. Diagn. 2 (2008) 11–20. [11] I.E. Tothill, Biosensors for cancer markers diagnosis, Semin. Cell Dev. Biol. 20 (2009) 55–62. [12] K.D. Robertson, DNA methylation and human disease, Nat. Rev. Genet. 6 (2005) 597–610.

[13] K. Ogi, M. Toyota, M. Ohe-Toyota, N. Tanaka, M. Noguchi, T. Sonoda, G. Kohama, T. Tokino, Aberrant methylation of multiple genes and clinicopathological features in oral squamous cell carcinoma, Clin. Cancer Res. 8 (2002) 3164–3171.

[14] L.F. Garcia-Melo, I. Álvarez-González, E. Madrigal-Bujaidar, E.O. Madrigal-Santillán, J.A. Morales-González, R.N. Pineda Cruces, J.A. Campoy Ramírez, P.D. Matsumura, M. de los A. Aguilar-Santamaría, N. Batina, Construction of an electrochemical genosensor based on screen-printed gold electrodes (SPGE) for detection of a mutation in the adenomatous polyposis coli gene, J. Electroanal. Chem. 840 (2019) 93–100.

[15] T. Hossain, G. Mahmudunnabi, M.K. Masud, M.N. Islam, L. Ooi, K. Konstantinov, M.S. Al Hossain, B. Martinac, G. Alici, N.T. Nguyen, M.J.A. Shiddiky, Electrochemical biosensing strategies for DNA methylation analysis, Biosens. Bioelectron. 94 (2017) 63–73.

[16] F. Gao, T. Fan, S. Ou, J. Wu, X. Zhang, J. Luo, N. Li, Y. Yao, Y. Mou, X. Liao, D. Geng, Highly efficient electrochemical sensing platform for sensitive detection DNA methylation, and methyltransferase activity based on Ag NPs decorated carbon nanocubes, Biosens. Bioelectron. 99 (2018) 201–208.

[17] A.C. Soares, J.C. Soares, V.C. Rodrigues, H.D.M. Follmann, L.M.R.B. Arantes, A.C. Carvalho, M.E. Melendez, J.H.T.G. Fregnani, R.M. Reis, A.L. Carvalho, O.N. Oliveira, Microfluidic-Based Genosensor to Detect Human Papillomavirus (HPV16) for Head and Neck Cancer, ACS Appl. Mater. Interfaces. 10 (2018) 36757–36763.

[18] M.D. Porter, T.B. Bright, D.L. Allara, C.E. Chidsey, Spontaneously Organized Molecular Assemblies. 4. Structural Characterization of n-Alkyl Thiol Monolayers on Gold by Optical Ellipsometry, Infrared Spectroscopy, and Electrochemistry, J. Am. Chem. Soc. 109 (1987) 3559–3568.

[19] R. Minghim, F. V. Paulovich, A. de Andrade Lopes, Content-based text mapping using multi-dimensional projections for exploration of document collections, Vis. Data Anal. 6060 (2006) 60600S.

[20] F. V. Paulovich, M.L. Moraes, R.M. Maki, M. Ferreira, O.N. Oliveira, M.C.F. De Oliveira, Information visualization techniques for sensing and biosensing, Analyst 136 (2011) 1344–1350.

[21] A.G. Lambert, P.B. Davies, D.J. Neivandt, Implementing the theory of sum frequency generation vibrational spectroscopy: A tutorial review, Appl. Spectrosc. Rev. 40 (2005) 103–145.

[22] X. Zhuang, P.B. Miranda, D. Kim, Y.R. Shen, Mapping molecular orientation and conformation at interfaces by surface nonlinear optics, Phys. Rev. B - Condens. Matter

Mater. Phys. 59 (1999) 12632–12640.

[23] H.S. Silva, P.B. Miranda, Molecular ordering of layer-by-layer polyelectrolyte films studied by sum-frequency vibrational spectroscopy, J. Phys. Chem. B. 113 (2009) 10068–71.

[24] R. Levicky, T.M. Herne, M.J. Tarlov, S.K. Satija, Using self-assembly to control the structure of DNA monolayers on gold: A neutron reflectivity study, J. Am. Chem. Soc. 120 (1998) 9787–9792.

[25] M.T.L. Casford, A. Ge, P.J.N. Kett, S. Ye, P.B. Davies, The structure of lipid bilayers adsorbed on activated carboxy-terminated monolayers investigated by sum frequency generation spectroscopy, J. Phys. Chem. B. 118 (2014) 3335–3345.

[26] C. Chung, M. Lee, Self-assembled monolayers of mercaptoacetic acid on Ag powder: Characterization by FT-IR diffuse reflection spectroscopy, Bull. Korean Chem. Soc. 25 (2004) 1461–1462.

[27] J.C. Miller, J.N. Miller, Basic statistical methods for analytical chemistry: Part I. Statistics of repeated measurements: A review, Analyst. 113 (1988) 1351–1356.

[28] C. Cai, Z. Guo, Y. Cao, W. Zhang, Y. Chen, A dual biomarker detection platform for quantitating circulating tumor dna (Ctdna), Nanotheranostics 2 (2018) 12–20.

[29] E. Povedano, E. Vargas, V.R.V. Montiel, R.M. Torrente-Rodríguez, M. Pedrero, R. Barderas, P.S. Segundo-Acosta, A. Peláez-García, M. Mendiola, D. Hardisson, S. Campuzano, J.M. Pingarrón, Electrochemical affinity biosensors for fast detection of gene-specific methylations with no need for bisulfite and amplification treatments, Sci. Rep. 8 (2018).

[30] P. Wang, H. Wu, Z. Dai, X. Zou, Picomolar level profiling of the methylation status of the

p53 tumor suppressor gene by a label-free electrochemical biosensor, Chem. Commun. 48 (2012) 10754–10756.

[31] X. Wang, F. Chen, D. Zhang, Y. Zhao, J. Wei, L. Wang, S. Song, C. Fan, Y. Zhao, Single copy-sensitive electrochemical assay for circulating methylated DNA in clinical samples with ultrahigh specificity based on a sequential discrimination-amplification strategy, Chem. Sci. 8 (2017) 4764–4770.

[32] S.H. Brewer, S.J. Anthireya, S.E. Lappi, D.L. Drapcho, S. Franzen, Detection of DNA Hybridization on Gold Surfaces by Polarization Modulation Infrared Reflection Absorption Spectroscopy, Langmuir 18 (2002) 4460-4464.

[33] B.M. Costa, C. Caeiro, I. Guimarães, O. Martinho, T. Jaraquemada, I. Augusto, L. Castro, L. Osório, P. Linhares, M. Honavar, M. Resende, F. Braga, A. Silva, F. Pardal, J. Amorim, R. Nabiço, R. Almeida, C. Alegria, M. Pires, C. Pinheiro, E. Carvalho, J.M. Lopes, P. Costa, M. Damasceno, R.M. Reis, Prognostic value of MGMT promoter methylation in glioblastoma patients treated with temozolomide-based chemoradiation: A Portuguese multicentre study, Oncol. Rep. 23 (2010) 1655–1662.

[34] M. Weller, R. Stupp, M.E. Hegi, M. van den Bent, J.C. Tonn, M. Sanson, W. Wick, G. Reifenberger, Personalized care in neuro-oncology coming of age: why we need MGMT and 1p/19q testing for malignant glioma patients in clinical practice, Neuro. Oncol. 14 (2012) iv100- iv108.

Figures

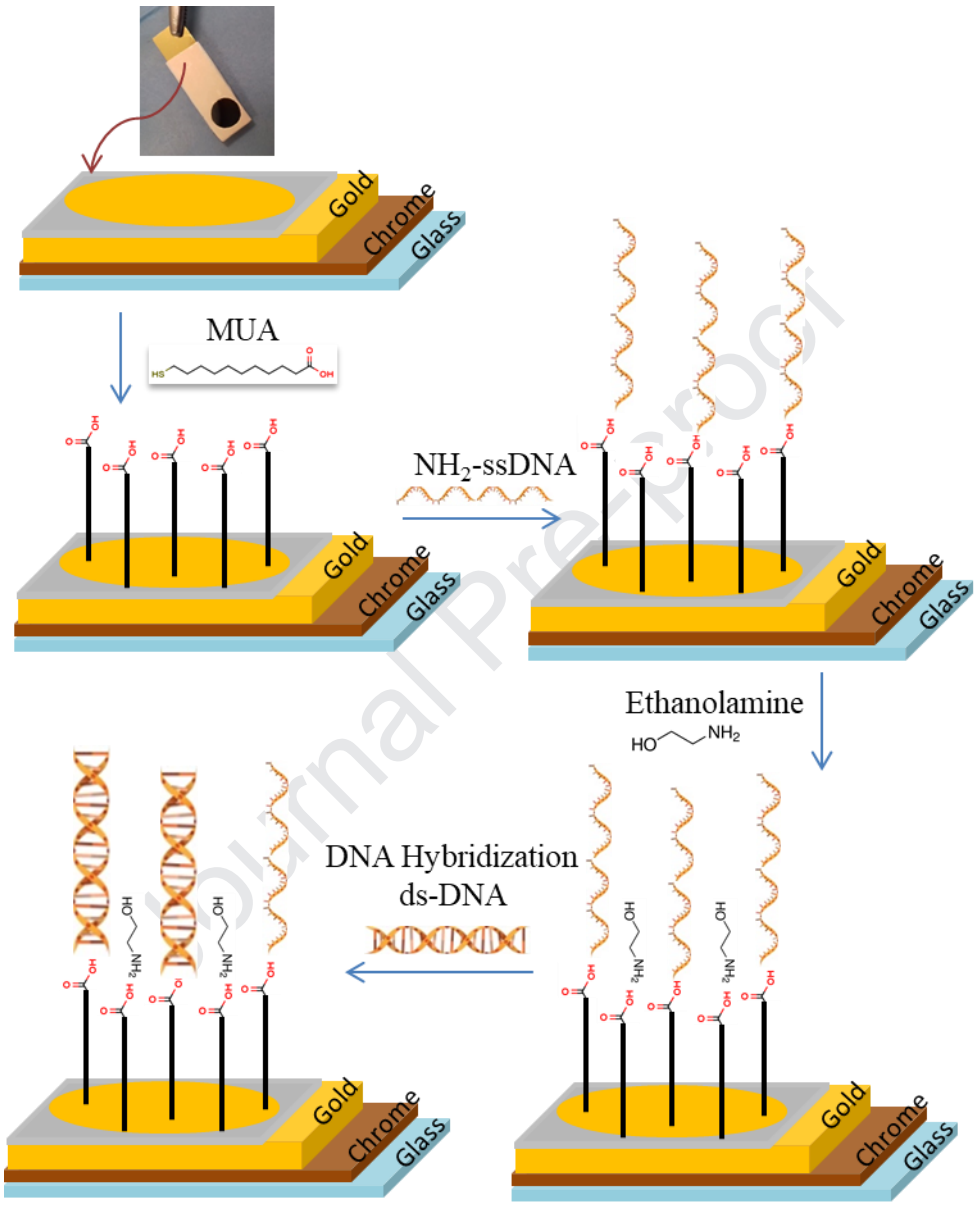

Figure 1: Schematics of the preparation of genosensors. A gold electrode is coated with a 11-MUA SAM film, onto which the NH_2-ssDNA probe was further adsorbed. This genosensor was treated with ethanolamine to avoid non-specific adsorption. The last picture shows the genosensor with its probe hybridized with its complementary sequence.

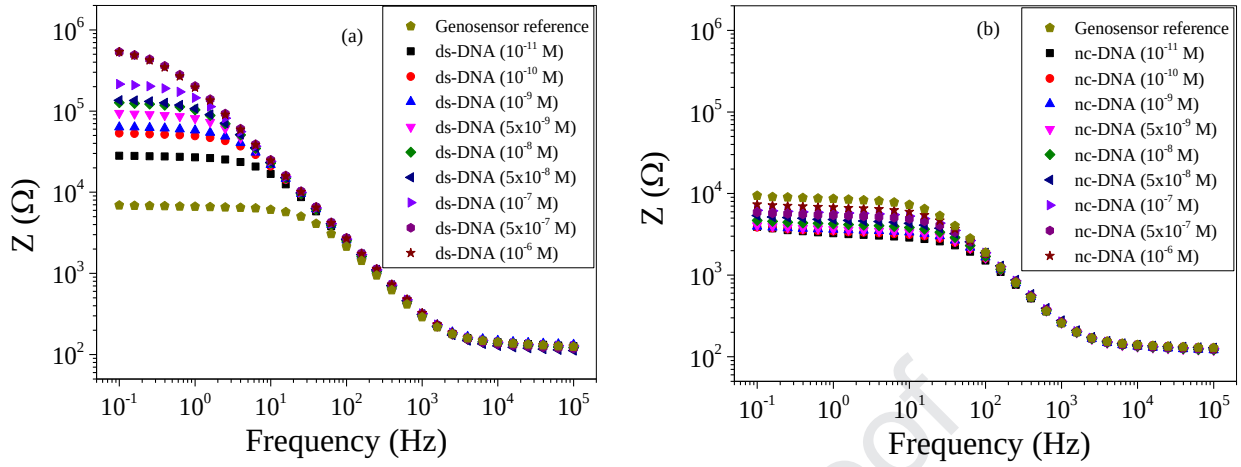

Figure 2: Impedance spectra for genosensors made with a MUA SAM monolayer prepared in ethanol, for different concentrations of the complementary sequence (ds-DNA) (a), and non-complementary sequence (nc-DNA) (b). The measurements were performed in 5 mM $[Fe(CN)_6]^{3-/4-}$ in PBS/$MgCl_2$ (1 mM).

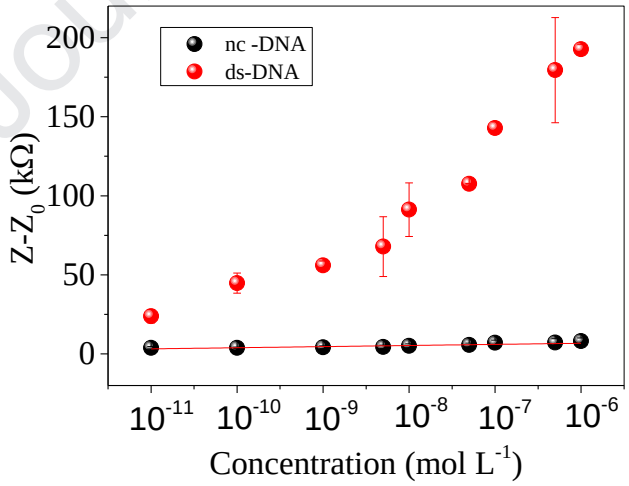

Figure 3: Analytical curves obtained from the electrochemical impedance spectra with $Z-Z_0$ at 1 Hz, for the complementary ds-DNA and non-complementary nc-DNA sequences.

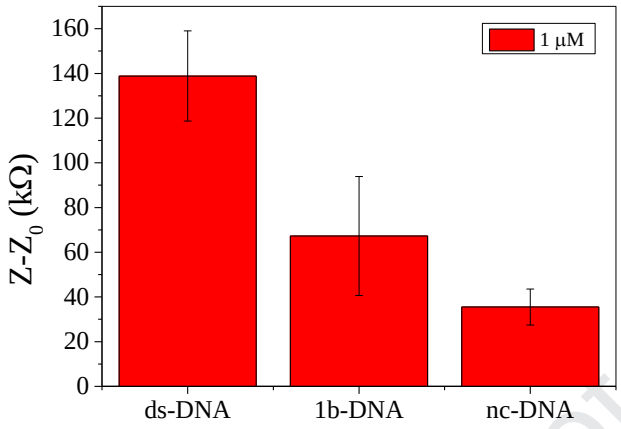

Figure 4: Change in impedance ($Z-Z_0$) at 1 Hz for samples at 1 µM of the DNA sequences (ds-DNA, 1b-DNA, nc-DNA). Electrochemical impedance measurements were performed in 5 mM potassium ferricyanide ($K_3[Fe(CN)_6]/K_4[Fe(CN)_6]$) in PBS/$MgCl_2$ (1 mM) with the genosensor made with an MUA SAM matrix.

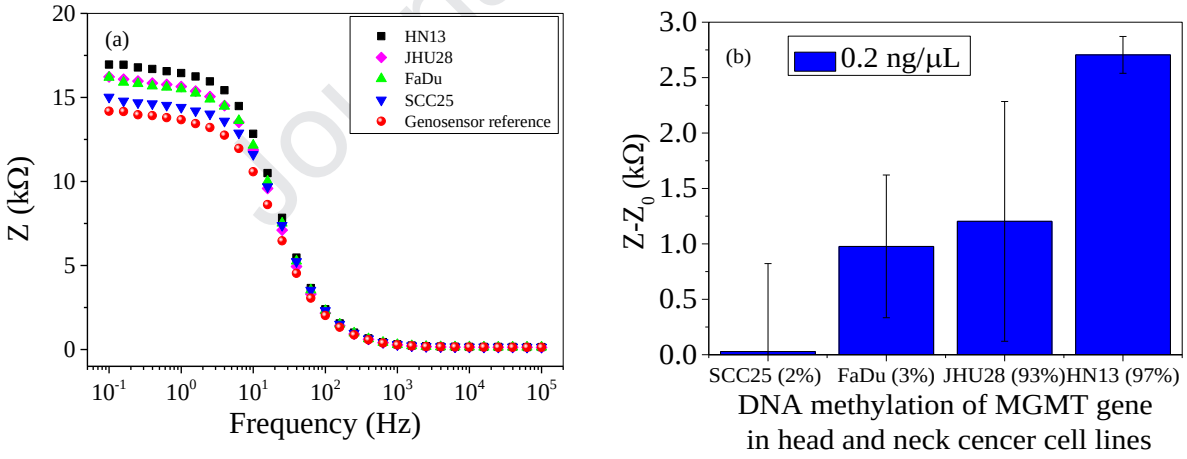

Figure 5: a) Impedance spectra for hybridization of the genosensor with 0.2 ng/µL DNA with distinct percentages of *MGMT* DNA methylation for the cell lines SCC25, FaDu, JHU28, and HN13. b) Change in impedance ($Z-Z_0$) at 1 Hz due to hybridization with 0.2 ng/µL DNA for cell lines with distinct percentages of *MGMT* DNA methylation (SCC25, FaDu, JHU28, and HN13).

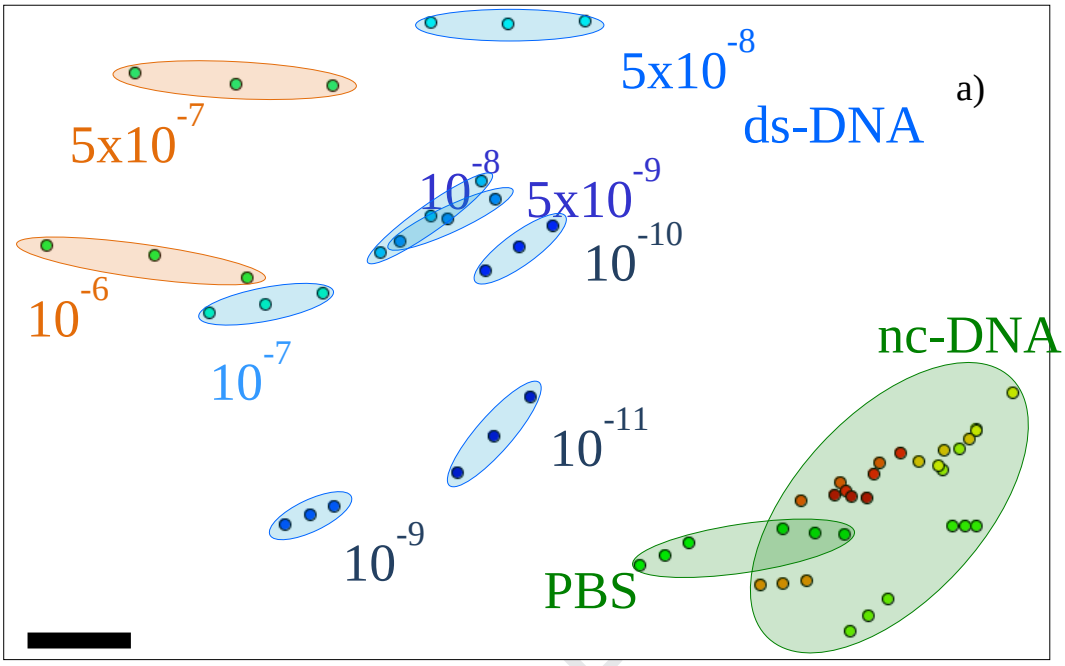
5x10-8
a)
ds-DNA
5x10-7
10-8
5x10-9
10-10
10-6
10-7
nc-DNA
10-11
10-9
PBS

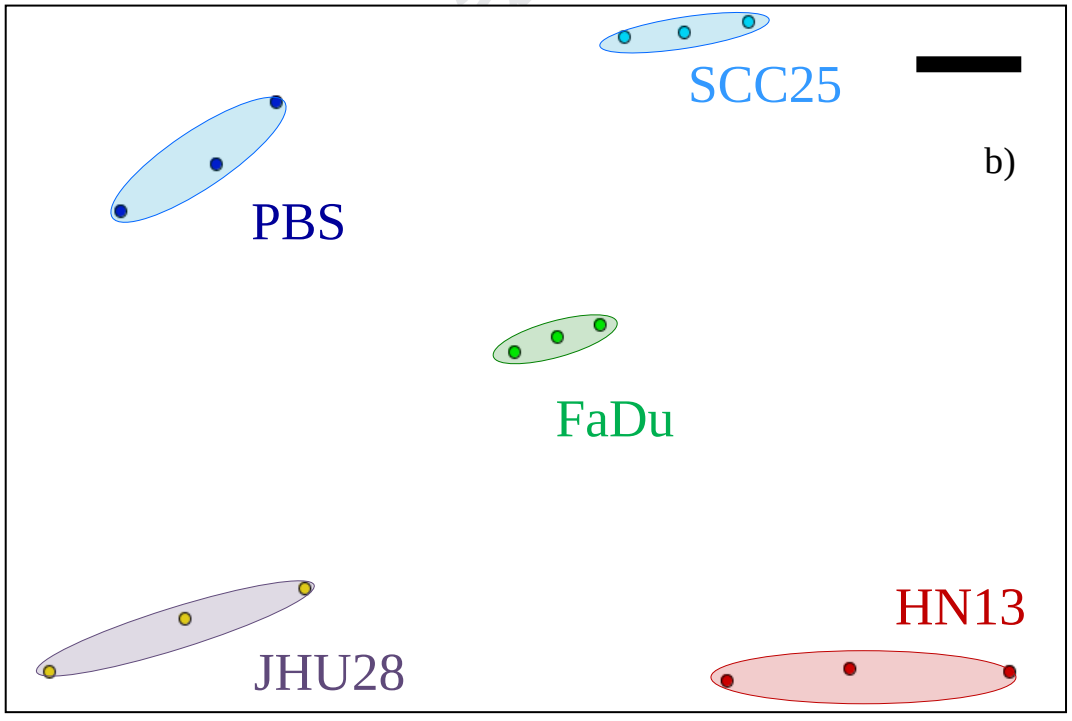
SCC25
b)
PBS
FaDu
HN13
JHU28

Figure 6: IDMAP maps obtained from the impedance spectra: (a) commercial samples (ds-DNA and nc-DNA) at various concentrations in PBS, (b) cell samples with distinct percentages of *MGMT* DNA methylation, namely SCC25, FaDu, JHU28, HN13.

Highlights

- Electrochemical genosensors to detect DNA methylation of the MGMT gene in head and neck cancer cell lines.
- Gold electrodes functionalized with self-assembled monolayers of acid mercaptoundecanoic (MUA).
- Detection limit was of 6.4 pM.